Carbon allocation dynamics in conifers and broadleaved tree species revealed by pulse labeling and mass balance

Forest Ecology and Management xxx (xxxx) 119258

Contents lists available at ScienceDirect

Forest Ecology and Management

journal homepage: www.elsevier.com/locate/foreco

Carbon allocation dynamics in conifers and broadleaved tree species revealed by pulse labeling and mass balance

Ido Rog*, Gilad Jakoby, Tamir Klein

Department of Plant & Environmental Sciences, Weizmann Institute of Science, Rehovot 76100, Israel

ARTICLE INFO

Keywords:
Carbon balance
Carbon allocation
Mean residence time
Flux partitioning
Root exudation

ABSTRACT

Fixed carbon (C) is a central resource, whose dynamic allocation by the tree determines its ability to establish, grow and compete with other species. Traditionally, tree C allocation has been estimated by isotopic or mass balance approaches. Here we developed a setup of $^{13}CO_2$ pulse-labeling, with a flux-coupled, three-phase detection, allowing us to follow C quantitatively. We examined C allocation patterns in 2-year-old potted saplings of five evergreen forest tree species that co-occur in a typical mixed forest in the Mediterranean region: two early succession conifers (*Pinus*, *Cupressus*) and three late succession broadleaf species (*Quercus*, *Ceratonia*, *Pistacia*). Across the five species, C moved from leaves to stem and fine roots following an exponential decay, with parameters that are consistent with the ecological role of each species. Eight days post-labeling, conifers allocated ~30% of the C belowground, and broadleaves <10%. In contrast, leaf C residence time was ~4 days in conifers and only ~1 day in broadleaves. Root exudation was quantified and shown to be small. We integrated our results into a compartmental model of ^{13}C distribution in the tree, enhancing our understanding of divergent C allocation strategies among tree species within the same ecosystem.

1. Introduction

How do trees from different species coordinate above- and belowground carbon (C) allocation (Enquist and Niklas, 2002; Poorter et al., 2012)? Biomass allocation have revealed a typical ratio between shoot and root growth rates (shoot/root ratio) (Wilson, 1988) that is species-specific and affected by phyto-geographical origins. In addition, environmental and ecological factors (e.g., successional stage) were shown to affect biomass allocation (Shukla and Ramakrishnan, 1984; Poorter et al., 2012). Defining C allocation dynamics is more complex in mixed species forest, where trees with different C allocation strategies co-occur in the same ecosystem (Sala et al., 2012; Klein et al., 2016) and it therefore requires individual scale tree C allocation resolution. One of the key parameters in understanding C allocation dynamics is the rate of C transfer from aboveground source compartments to belowground sink compartments, which is in the range of several days (Epron et al., 2012). Environmental factors together with species-specific parameters were found to influence the lag time more than the transfer path *per se* (Högberg et al., 2008; Dannoura et al., 2011; Kuptz et al., 2011). Moreover, aboveground and belowground pools are insufficient to fully understand whole-plant C allocation, which should also include pools and fluxes of different compartments. These limitations raise the importance of understanding the short-term C allocation dynamics (i.e. several days) of different tree species sharing the same ecosystem.

The challenge in studying whole plant C allocation is to follow the different fluxes and pools simultaneously. C allocation can be separated into the C flux that transports between sinks to storage compartments, and the C pool in every compartment. C allocation can be estimated by C mass balance approach, applying biomass measurements together with respiratory CO_2 efflux measurements (Klein and Hoch, 2015). However, small internal and external C fluxes (e.g. exudation) are potentially masked by the major fluxes (e.g. respiration) and are difficult to measure directly. Artificial C labeling, using stable $^{13}CO_2$ as short-term pulse labeling of the whole plant (Keel et al., 2006; Sangster et al., 2010) or plant parts (Streit et al., 2013) provide high-resolution information on recently assimilated C allocation (Schnyder et al., 2003). The high isotopic signal can be detected in different plant tissues, as well as other forest ecosystem components such as soil and microbial communities (Brant et al., 2006; Epron et al., 2012). Using this high resolution, the plasticity of C allocation strategies can be detected in the different growth stages of the plant (Wegener et al., 2015) and even the metabolic compound being stored (Desalme et al., 2017), together with the effect of environmental factors. The complex methods to measure the entire fluxes and pools in the different compartments to-

* Corresponding author.
E-mail addresses: ido.rog@weizmann.ac.il (I. Rog), gilad.jakoby@weizmann.ac.il (G. Jakoby), tamir.klein@weizmann.ac.il (T. Klein).

https://doi.org/10.1016/j.foreco.2021.119258
Received 6 December 2020; Received in revised form 7 April 2021; Accepted 9 April 2021
0378-1127/

gether with the wish to explore the impact of abiotic factors, encourage scientists to use models (Franklin et al., 2012; Merganičová et al., 2019) and specifically compartmental models (Epron et al., 2012) to describe the C allocation dynamics without direct measurements.

Tree species and environmental factors influence C allocation strategy in terms of C use and storage in the diurnal and annual timescales. Preferential allocation of fresh C can be affected by seasonal periodicity. For example, in temperate trees, most of the spring photoassimilated C is allocated to stem, in agreement with early wood formation (Klein et al., 2016). On the other hand, root exudation occurs in the autumn in temperate trees and in the dry season in Mediterranean trees (Jakoby et al., 2020). Extreme environmental conditions also affect tree C allocation dynamics directly and in a short time scale, for example during drought (Ruehr et al., 2009). In such conditions, trees prioritize the allocation of recently assimilated C to belowground fluxes (Hagedorn et al., 2016). However, elevated temperatures commonly enhance aboveground C allocation to growth (Way and Oren, 2010), due to increase in plant respiration (Atkin and Tjoelker, 2003), and to soil efflux (Blessing et al., 2015). Understanding the response of various tree species to disturbances such as elevated temperature can improve our ability to predict forest trees' response to climate change. Still, quantitative measurements of C allocation among tree compartments in the Mediterranean species that are exposed to harsh environmental conditions and vulnerable to climate change (Giorgi and Lionello, 2008; Alessandri et al., 2014) are currently lacking.

Here we examined the C partitioning strategies of potted saplings of five different widespread species co-occurring in forests around the Mediterranean region. In particular, we were interested in interspecific differences and the proportion between aboveground and belowground C allocation of the different species. To follow C quantitatively, and study its distribution between the different sinks, we developed a CO_2 labeling and detection setup using a stable ^{13}C isotope. By using a $^{13}CO_2$ pulse-chase experiment with mass and flux measurements, we enhance the resolution of the labelled C detection, allowing the measurement of small C fluxes at high temporal resolution. We measured the three main short-term C sinks: respiration, biomass pool, and root exudation. We enhanced our quantification of C kinetics by using a compartmental model of ^{13}C distribution in the tree. The model described the continuous and linear flux rates (i.e., the compartment fluxes are expected to be related to the amount of C in the tissues) however unique species-specific C allocation fluxes are not characterized by the model and stand out. We hypothesized that (1) C allocation strategies should diverge in phylogenetically distant tree species; (2) C will be distributed to above/belowground sinks differently among the five species according to their succession processes or functional groups.

2. Materials and methods

2.1. Plant material and growth conditions

Two-years-old saplings (diameter 0.5–1.5 cm; $n = 3$ per species) of *Quercus calliprinos* Webb, *Ceratonia siliqua L.*, *Pistacia lentiscus L.*, *Pinus halepensis* Miller and *Cupressus sempervirens L.* were taken from a Forest Service nursery (KKL, Jewish National Fund, Eshtaol, Israel) and planted in 2 L pots (Fig. S1, Table S1). All five species are evergreen; *Pinus* and *Cupressus* are conifers, whereas the others are broadleaved. The species were selected for being among the dominant tree species in the East Mediterranean forest and maquis. Among the many tree species in this forest biome, *Pinus* and *Quercus* are typically the dominant genera. *Pinus* and *Cupressus* are characterized by traits of early succession species, such as fast growth and massive seed production (Delipetrou et al., 2008; Sheffer, 2012). In contrast, our *Quercus*, *Ceratonia* and *Pistacia* species are characterized with late succession properties such as low growth rate, shade tolerance and longer lifecycle (Ne'eman and Izhaki, 1996; Bonet, 2004; Maestre et al., 2004; Sheffer, 2012).

Soil from Harel forest (31°43′30.9″N 34°57′38.8″E), where all species are naturally co-occurring, was mixed with sand in a ratio of 1:4 to preserve the naturally occurring fungi and bacteria in the media. Saplings were grown for four months in a glass greenhouse (light shading of ~25%, temprature was controled by aircondition at ~25 °C; no humidity control) on the Weizmann Institute of Science campus (Rehovot, Israel) and irrigated (manual irrigation, every 3–4 days). Environmental conditions around Rehovot during March-July 2017 were: overall minimum and maximum temperatures of 8.0 °C and 38.3 °C, average temperature at night 19.6 °C and day 25.2 °C, average mid-day global light intensity of 800.2 $W \times m^{-2}$, average midday relative humidity of 50.1% and average midday VPD 2.02 kPa (Beit-Dagan meteorological station, 10 km North of the research institute). After labeling and during the measurements, trees were located in the Weizmann institute garden under ambient conditions (conditions during the 8 days post labeling): minimum and maximum temperatures of 23.3 °C and 33.2 °C, average light intensity of 858.6 $W \times m^{-2}$ and average midday relative humidity of 55.6%.

2.2. General experimental design

A setup of isotopic labeling followed by pools and fluxes measurements in different compartments was developed (Fig. 1). For labeling, a controlled atmosphere sealed chamber equipped with a top high light lamp was connected to $^{13}CO_2$ labeling and detection systems (For further details see "*$^{13}CO_2$ labeling and detection*"). Saplings of 5 different Mediterranean species were labeled and intensively measured once a day following labeling. Measurements were separated into pools and fluxes of three plant compartments: leaves (mature, large leaves), lateral shoots (representation to all woody tissues aboveground) and fine roots (lateral, 1st −2nd order, ~5–10 cm long, representation to the sapling root system) for holistic C balance. For C balance analysis, the total amount of labeled C entering the plant was quantified using two methods: Assimilation rate during the labeling; and biomass sampling immediately after the labeling period (For further details see "*$^{13}CO_2$ labeling and detection*"). Description of the different methodologies appears in the next sections below.

2.3. $^{13}CO_2$ labeling and detection

A total of 15 potted saplings, three per species, were pulse-labeled (July 2017) for three hours. The soil surface was covered with a plastic bag to prevent label transfer by dark fixation or diffusion to the roots. A consistent close atmospheric control chamber (0.90 × 0.65 × 0.60 m; COY, MI, USA) was equipped with a top, high light LED lamp (Agro light, Beit Yehoshua, Israel) modified to photosynthetically active radiation, PAR, of 700–1000 μmol m^{-2} sec^{-1} (inside the chamber in different heights of the foliage). The conditions in the sealed chamber were regulated using two main components: (1) humidity control: by ultrasonic humidifier (uses high-frequency sound vibrations to produce extra fine water droplets) and a chemical desiccant. (2) Temperature control: by electrical heating and cooling systems. Steady conditions of 25 °C and 60% relative air humidity were stabilized and homogenized in the chamber by continuous air movement using a pump and vent. The desired concentration of $^{13}CO_2$ was created using labeled sodium bicarbonate (^{13}C, 99%, Cambridge Isotope laboratories, Tewksbury, MA, USA) dissolved in 50% HCl (Fig. S2). This was achieved after initial flush of $^{12}CO_2$ out of the chamber using Zero air (air continuing no CO_2) and pure N_2 (99.99%) for maintaining $^{12}CO_2$ levels < 50 ppm for a few minutes only (Fig. S2). All ^{13}C measurements were performed using a ^{13}C cavity ring down spectroscopy analyzer (CRDS) (Picarro G2131i, Picarro, Santa Clara, CA, USA) (< 0.1‰ precision, < 0.5‰ drift for $\delta^{13}C$ in CO_2) and a closed system measurement package (Picarro A0701/2). Stabilized conditions of 400 ± 150 ppm of $^{13}CO_2$ were maintained in the sealed chamber for the duration of the three-hours of pulse labeling.

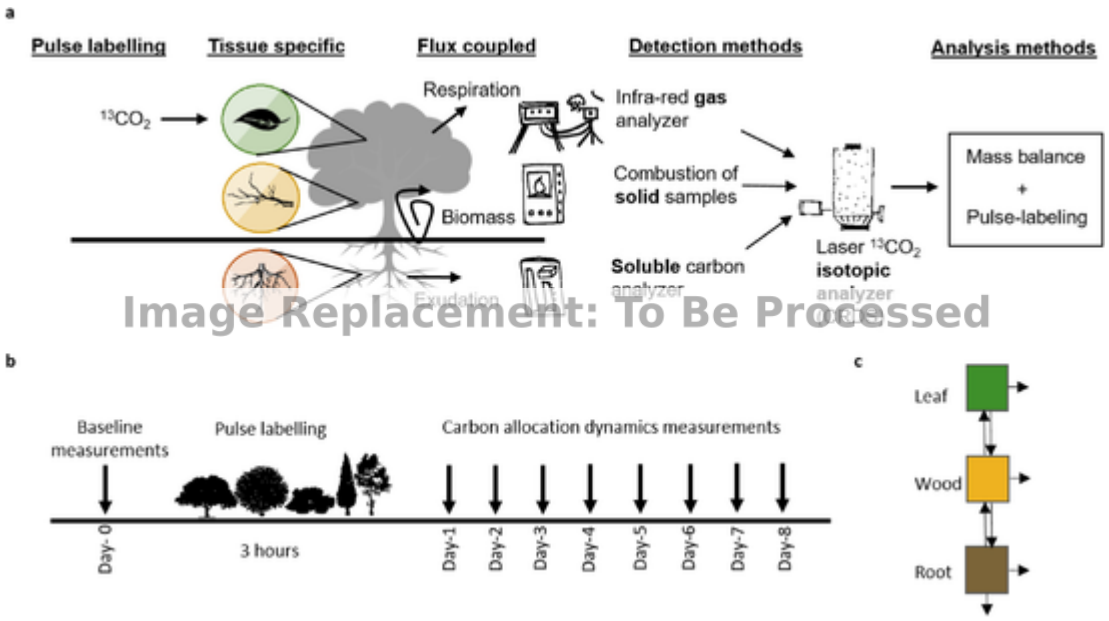

Fig. 1. Schematic representation of our methodology and experimental design. (**a**) Carbon allocation dynamics were measured by $^{13}CO_2$ pulse labeling and tissue specific, flux coupled, and three-phase detection method. For clarification, ^{13}C was measured in respiration and biomass of each of the tree compartments (leaves, stem and branches, and roots). (**b**) Schematic experimental design for the potted labeling and carbon allocation measurements. One day before the labeling, flux measurements and biomass samples were taken to be used as a baseline. For labeling, a continuous atmospheric control chamber was connected to $^{13}CO_2$ labeling and detection systems. Saplings of 5 different Mediterranean species were labeled and intensively measured once a day following labeling. All pools were converted into mg C day^{-1} $sapling^{-1}$, for a species-specific carbon balance analysis. (**c**) Schematic representation of the compartmental model of C pool distribution in the tree. Measured carbon allocation dynamic compared to the compartmental model outpost.

In order to expose all the trees to equal conditions without overcrowding the sealed chamber, saplings were divided into two consecutive labeling batches. Immediately after labeling, subsamples from each plant compartment were taken to determine the amount of initial fixed ^{13}C entering the plant (For further details see the "*biomass sampling*" section).

2.4. Gas exchange measurements

To quantify the amount of labeled ^{13}C respired from specific tissues of each sapling, we measured the dark respiration flux rate and C isotopic ratio, simultaneously. Respiration of the different tissues was measured by a portable photosynthesis, infra-red gas analyzer (IRGA; GFS-3000, Walz, Effeltrich, Germany). The gas flux of the IRGA was analyzed with a CO_2 analyzer (Picarro G2131i) which was directly interfaced to the exhaust ventilation of the IRGA module and simultaneously measured the ratio of $^{13}CO_2$ and $^{12}CO_2$ isotopes from the respired CO_2. Because the exhaust ventilation of the IRGA produced higher flow rate than needed for the isotopic analyzer inlet, an open valve was integrated, from which extra flow was released. Standard leaf chamber (Walz 3010-S) with top LED light source (Walz 3040-L) were set to zero light. The CO_2 level was set to provide a stable concentration of 400 ppm; flow rate was set to 750 μmol s^{-1}; and the impeller to speed 7. Saplings were covered for 30 min for dark adaptation and a single intact (connected) mature leaf from the broadleaves trees, or a group of 10 adult needles from *Pinus* and mature scales from *Cupressus*; disconnected lateral shoot (~3 cm length, non-photosynthetic shoots); or disconnected root (lateral, 1st –2nd order, ~5–10 cm long, cleaned by rapid nitrogen gas pressure) was inserted to the IRGA chamber and measured. All measurements were taken after the IRGA and the CRDS values were stable. Leaves were sampled during the morning (10:00–12:00) and fine roots were sampled in the afternoon (12:00–14:00).

In addition to respiration, the rate of net photosynthesis was measured once a day prior to labeling to estimate the total amount of assimilated ^{13}C during labeling. Conditions inside the IRGA chamber were set similarly to the dark respiration measurement (CO_2 400 ppm; flow rate 750 μmol s^{-1}; impeller speed 7; no temperature or humidity control), with additional photosynthetically active radiation, (PAR) of 700 or 1000 μmol m^{-2} s^{-1} (according to the plant's distance from the light source during labeling (Table S2).

2.5. Biomass sampling

Leaf, woody tissues and fine root tissues were sampled 24 h before, immediately after, and once a day following labeling of each sapling. To minimize sampling damage to saplings, the same tissues used for respiration measurements, were used for biomass measurements (one leaf, few needles or root branchlet (2nd –3rd order roots) ~ 1% of the compartment in every sampling). All saplings, mainly of the late succession species (*Quercus*, *Ceratonia* and *Pistacia*) have relatively low growth rate and thus low number of branches. Sampling woody tissues intensively would have caused damage to the entire sapling and affected the carbon allocation measurements and interpretation. Sample sizes were kept as small as possible, therefore woody tissues' (branches carrying bark, representing whole woody shoot) sampling was skipped in some of the days. Similarly, biomass leaves and roots samples were skipped in day 6 and 7. Leaves were sampled during the morning (10:00–12:00) and fine roots were sampled in the afternoon (12:00–14:00). Samples were oven-dried at 60 °C for 48 h and kept dry until further analysis. An amount of 1 mg of dry tissue biomass (leaves, woody tissues (whole branch, including phloem), or fine roots), not grinded (for reducing contamination), with three technical replicates, was weighed in a tin capsule and installed onto a combustion module equipped with an auto-sampler (ECS 4010, Costech Analytical, Valencia, CA, USA). The resultant CO_2 gas product was analyzed with the ^{13}C analyzer, which was directly interfaced to the combustion module (Fig. 1). Results were expressed as parts per thousand (‰) deviations from the international C isotope standard (Vienna Pee Dee Belemnite, VPDB). Three replicates from each biological sample were measured and averaged to minimize

variance related to local tissue patches, and to better represent the entire plant compartment. An international standard (IAEA-CH-3 (-24.724‰), Cellulose, International Atomic Energy Agency, Vienna, Austria) (Verkouteren, 2006), (IAEA-303, 93.3‰ and 466‰) (Parr and Clements, 1991) was used and internal standards (homogeneous Spirulina powder with a ^{13}C of −29.2‰) and Glucose (Sigma) −11.1‰) were used every 9 samples. In addition, standard samples of C amount (Acetanilide C_8H_9NO and Atropine $C_{17}H_{23}NO_3$, Costech Analytical) were used for calculating the amount of C present in each sample.

2.6. Area and mass of sapling compartments

Area and mass of the different plant compartments were measured following the 8 days of C balance measurements. Saplings were divided into the three compartments (Leaves, aboveground woody tissues and roots). Surface area of each compartment was measured by a tabletop scanner (MFP-M477fdh, HP, CA, USA) and analyzed by ImageJ software (Rueden et al., 2017) using threshold tool and area calculation. Next, samples were oven-dried at 60 °C for 48 h and kept dry until dry mass measurements. For samples with extremely large surface area (i.g. conifers' fine roots, conifers' needles, *Pistacia* fine roots) a ratio between areas to mass was calculated for three subsamples and the average ratio was multiplied in order to upscale to the total sapling compartment area. Area and mass values of the samples from all the measurements (total of 10 days) were added to compute the total area and mass value of each sapling compartment.

2.7. Root exudation sampling and analysis

Root exudates were collected from intact lateral fine roots using a non-soil syringe system modified from Phillips et al. (2008) for measuring exudation flux. Eight days after labeling two to three fine roots of each sapling were excavated (representative to high-branched fine roots), washed in double distilled water (DDW) and inserted into a 20 ml syringe filled with glass beads (5 mm). The intact root was incubated with 10 ml DDW for 24 h. Next, liquids were sucked out and filtered immediately thorough a 0.22 μm sterile syringe filter (Millex PVDF, Millipore Co., Billerica, MA). Samples were separated into two: (1) C isotope analysis: samples were lyophilized (Gamma 2–16 LSCplus, Christ, Osterode am Harz, Germany) to a completely dry pellet, and 1 mg of the pellet was weighted in tin capsuls and measured using the combustion module and the ^{13}C analyzer (Picarro G2131i), similarly to the biomass measurements (Further information in "*biomass sampling*"). (2) Exudation amount determination: Half of the solutions were analyzed for dissolved organic C on a total organic C analyzer (TOC; Shimadzu TOC-L CPH/CPN; Shimadzu Scientific Instruments, Kyoto, Japan). Additional two control samples were collected: (1) From unlabeled saplings species for isotopic baseline; and (2) From samples with no root in the syringe for the organic material background in the solution. Samples from unlabeled *Quercus* and *Cupressus* were not collected and the average value of the other three tree species was used as a control value (Table S4).

2.8. C allocation calculation

Isotopic composition of the different pools and fluxes are presented in δ-notation in per mill units (‰) relative to the VPDB standard. $\delta^{13}C$ values were transformed into atom fraction as contribution of ^{13}C atoms number to the total C atoms (Coplen, 2011). Calculating atom fraction (AF) was as follows:

$$AF = \frac{100 \times VPDB \times \left(\frac{\delta 13C}{1000} + 1\right)}{1 + VPDB \times \left(\frac{\delta 13C}{1000} + 1\right)} \quad (1)$$

where VPDB is the standard value for the isotope ratio of the Vienna Pee Dee Belemnite (0.0111802).

The units of the total amount of ^{13}C originating from the pulse-labelling were standardized separately for the different plant pools and fluxes. The pools units (i.e. mg ^{13}C compartment^{-1} day^{-1}) were obtained using the following equations (Eq. 2–6):

$$Res^{13}C = \frac{AF^{tx} - AF^{tz}}{100} \times Flux \times Area\,(total) \times t \quad (2)$$

where atom fraction time zero (AF^{tz}) values were taken prior to labeling and atom fraction time x (AF^{tx}) are samples taken on a day-x post labeling (both values are related to the baseline value of an empty chamber). *Flux* is the dark respiration flux (μmol CO_2 m^{-2} s^{-1}) of the specific tissue (leaves/woody tissues/roots); *Area (total)* (m^2) is the total area of the respected tissue in each sapling; *t* is the up-scaling of the flux to total amount per day (86400 sec day^{-1}) assuming equal respiration flux during day and night in the same temperature (Farquhar and Busch, 2017); values converted from μmol CO_2 to mg C by (multiplying by 0.012). Normalization of respiration rate to temperature of 25 °C and upscaling to average daily temperature ($Res_{corrected}$) was calculated according to Eq. (3):

$$Res_{corrected} = Res^{13}CxQ_{10}^{\frac{T-25^oC}{10}} \quad (3)$$

where $Res^{13}C$ is the respiration rate measured at 25 °C. Q_{10} value was taken from the observed temperature dependence, where *T* is the average temperature during the 8 days of measurements (Fig. S3; Table S3).

For calculating the allocation of ^{13}C into biomass, we followed Eq. (4):

$$Biomass_{pool}{}^{13}C = \frac{AF^{tx} - AF^{tz}}{100} \times Mass\,(total) \times \%C \quad (4)$$

Values of samples prior to labeling were used as atom fraction in time zero (AF^{tz}) and samples taken post labeling were used as atom fraction time x (AF^{tx}). *Mass (total)* is the total biomass of the specific tissue (leaves/woody tissues/roots; mg) in a specific sapling, assuming no changes except of the sacrificed parts. For the timeframe of the experiment, i.e. 8 days, biomass increment through tissue growth, and biomass loss, through litter production, were assumed neglectable (i.e. no growth or tissue loss). The *% C* in each sample was analyzed by the CRDS and multiplied by the aforementioned components. For biomass change rate calculations, the biomass pool of day *t* was subtracted from day *t-1* separately for the different tissues.

Root exudation rates and their ^{13}C allocation were calculated using the following equations:

$$Exu_{rate} = \frac{Exu^{labelld} - Exu^{control}}{Root\ area \times t} \quad (5)$$

Exudation rates (Exu_{rate}) were calculated as the total amount of C exuded from each root system. $Exudation^{control}$ is the amount of organic C in a control collection tube, (without root) (mg); $Exudation^{labeled}$ is the amount of organic C in a collection tube with intact root (mg); *t* is the incubation period (days); *Root area* is the root surface area (cm^2) of the investigated root strand.

Exudation ^{13}C ($Exu^{13}C$) values were calculated using the equation:

$$Exu^{13}C = \frac{AF^{tx} - AF^{tz}}{100} \times Exu_{rate} \times Area\,(roots) \quad (6)$$

where parameters are as in Eq. (4); exudation rate was calculated from Eq. (5); *Area (roots)* is the total root area of the individual sapling (cm^2).

Estimation of mean residence time and half-life times of the ^{13}C in leaves was calculated by:

$$N(t) = N_0 e^{(-\lambda t)} \quad (7)$$

where N_0 is the initial amount of pulse-labeling originated ^{13}C in leaves immediately after labeling occurred; λ is the decay constant; $N(t)$ is the quantity of labeled C at a given time. Mean residence was calculated as $1/\lambda$ and the half-life time was calculated as $t_{1/2} = \ln(2)/\lambda$. Verification of the whole set of calculations (units conversion, conifers size upscaling) was tested by calculating both parameters twice: first by using the $\delta^{13}C$ values, and second by using the total amount of pulse-labeling originated ^{13}C, after transformation to mg ^{13}C leaves^{-1} day^{-1} units.

2.9. Whole-tree C balance calculations

C fluxes were calculated from independent measurements of three saplings from each species to form a whole tree C balance for the 8 days' post-labeling period. The total amount of labeled C which entered the sapling (samples taken after 3 h of labeling) was used for the total C budget for each species. This value was verified by comparing with an additional method of calculating the assimilation rate during labeling. Assuming no additional influx of labeled C after labeling (re-fixation of respired $^{13}CO_2$), the mean of the total budget of C in any day following labeling was estimated by subtracting the mean pool accumulation (in absolute values, respiration (leaves, woody and roots) and exudation from roots) from the C budget in the previous day. Each of the C pools (respiration, exudation and biomass) was measured independently on a daily basis post labeling. Daily changes in pools (measured once a day) were converted into mg C day^{-1} sapling^{-1} units, and daily means were integrated into a C balance, species-specific, dataset (Table S9). Aboveground woody tissues' biomass pool and respiration (stem efflux) were measured only on days 2 and 4 (*Cupressus* only in day 2), and were estimated on the other days; ^{13}C allocation into aboveground woody tissues' biomass was estimated each day to complete the C balance, and samples from day 2 were used to calculate the labeled respiration ratio of the woody tissues (i.e., the ratio between the amount of labeled C in a respiration pool and that in a certain biomass sample). The ratio between the amount of labeled C in root biomass and the exudation flux was calculated on day 8 only.

2.10. Statistical analysis

Statistical analysis was done using R and the interface R Studio (Team, 2018). We used repeated-measures ANOVA to test for differences among tree species (5 species (fixed), 3 replicates of each (random)), within days of measurement (before, immediately after labeling and 5-time points following the labeling (fixed)), and within tissues of each plant (leaf or root) (fixed) and the interactions between them in the $\delta^{13}C$ values and in the total C day^{-1} sapling^{-1} units (Package *stas* (version 3.6.1) and *car* (version 3.0)). Logarithmic transformation has modified to the $\delta^{13}C$ and C day^{-1} sapling^{-1} units to conform a quasi-normal distribution. For testing the significant effect between early and late succession species in individual days (before labeling and 8 days after labeling) we used *t*-test and Bonferroni correction for the multiple comparison applied (Using *stats* package) (Table S5). Expected exponential decay curves representing C movement from leaves to stem and roots were calculated using the non-linear least square function (Package *stats* version 3.6.1) (Fig. 2 & Fig.3). Values of *p-value for* N_0 and λ (the two estimated parameters in the exponential curve) are presented in Table 1 & S8. Calculation of the two estimated parameters for individual saplings and averaging them yielded similar values Table S10.

2.11. Compartmental model of ^{13}C distribution in the tree

We employed a mechanistic tree compartmental model of C distribution to complement and extend our empirical approach. We used a "box-model" (Epron et al., 2011; Epron et al., 2012) to investigate how a set of fluxes and initial conditions affect the pools dynamics of the different compartments. The model is based on three compartments (Leaf (*L*), Woody tissues (*W*), and Root (*R*)) and two additional sinks, atmosphere (*Atm*) and soil (*S*), for the respiration and exudation fluxes, respectively. Three components were used for the model: First, ordinary differential equations: Mathematical expressions specify the amount of C in each of the compartments changes as a function of the magnitude of each flow in terms of time (Table S6).

$$\frac{di}{dt} = \pm k(i:j) * A(i) \quad (8)$$

where di/dt is the mathematical expression (box i in time t) of the amount of C in each of the compartments change (k), where the flux denoted by Ki:j is read as from box i to box j, as a function of the magnitude of each flow (A).

Second, flow parametrization: Assuming linear fluxes, the various rate coefficients were taken from the empirical measurements (calculated the average rates (day 1–8 post labeling) (Table S7).

$$k_{i:j} = \frac{F^t_{i:j}}{M^t_i} \quad (9)$$

where M^t_i is the mass of box i in time t and $F^t_{i:j}$ is the flux rate calculated from box i to box j.

Third, initial conditions: Empirical initial ^{13}C mass of the different compartment pools immediately after ^{13}C pulse labeling (assuming no re-fixation of the labelled CO_2) (Table S7). Finally, Mathematical algorithm (ode45, MATLB solver) (Dormand and Prince, 1980; Shampine and Reichelt, 1997) was used for solving the differential equations. For temperature sensitivity of the model, different warming scenarios were tested (+5°C and + 10 °C) for calculating the various rate coefficients that averaged (days 1–8 post labeling) and entered to the model.

3. Results

3.1. Assimilation of $^{13}CO_2$

Saplings were allowed to photosynthesize for three hours at a ~99% $^{13}CO_2$ environment (at 250–450 ppm $^{13}CO_2$) under high light conditions (PAR of 700–1000 μmol m^{-2} s^{-1}, representing the range of light level across the saplings' crowns) and optimal temperature and humidity (see Materials and Methods). Rates of net photosynthesis were moderate for the study species, on average 4.27 ± 1.63 μmol CO_2 m^{-2} s^{-1} across saplings and the light levels (Table S2). Interspecific differences were small, but *Pistacia* showed rates higher than 5 μmol CO_2 m^{-2} s^{-1} at PAR of 700 μmol m^{-2} s^{-1} (Table S2). In contrast, leaf area varied widely among the species, and primarily between the typically taller conifers saplings, and the shorter broadleaf saplings (Table S1). Differences in leaf area caused high variability in the amount of fixed $^{13}CO_2$, with up to 3-fold increase in ^{13}C uptake in *Cupressus* vs. *Quercus* (Fig. S4, Table S1). In addition, after labelling, the two conifers and *Pistacia* allocated part of the ^{13}C to the branches while in *Quercus* and *Ceratonia* most of the ^{13}C remain in the leaves (Fig S4). Following pulse labeling, we were able to use these estimates and follow quantitatively the ^{13}C distribution in the different sapling sinks.

3.2. $\delta^{13}C$ of leaves, branches and roots

Saplings from different species allocated different amounts of ^{13}C among the compartments in the different days after labeling. When comparing the interaction between the tree species, and the time of measurement, there was a significant effect (Species:Day, Repeated-measures, ANOVA, $F_{28,150} = 2.7$, $p < 0.001$, Table S5). Prior to labeling, fine roots of all saplings were significantly enriched with ^{13}C compared to leaves, −26.6 ± 0.3‰ and −28.3 ± 0.3‰, respectively

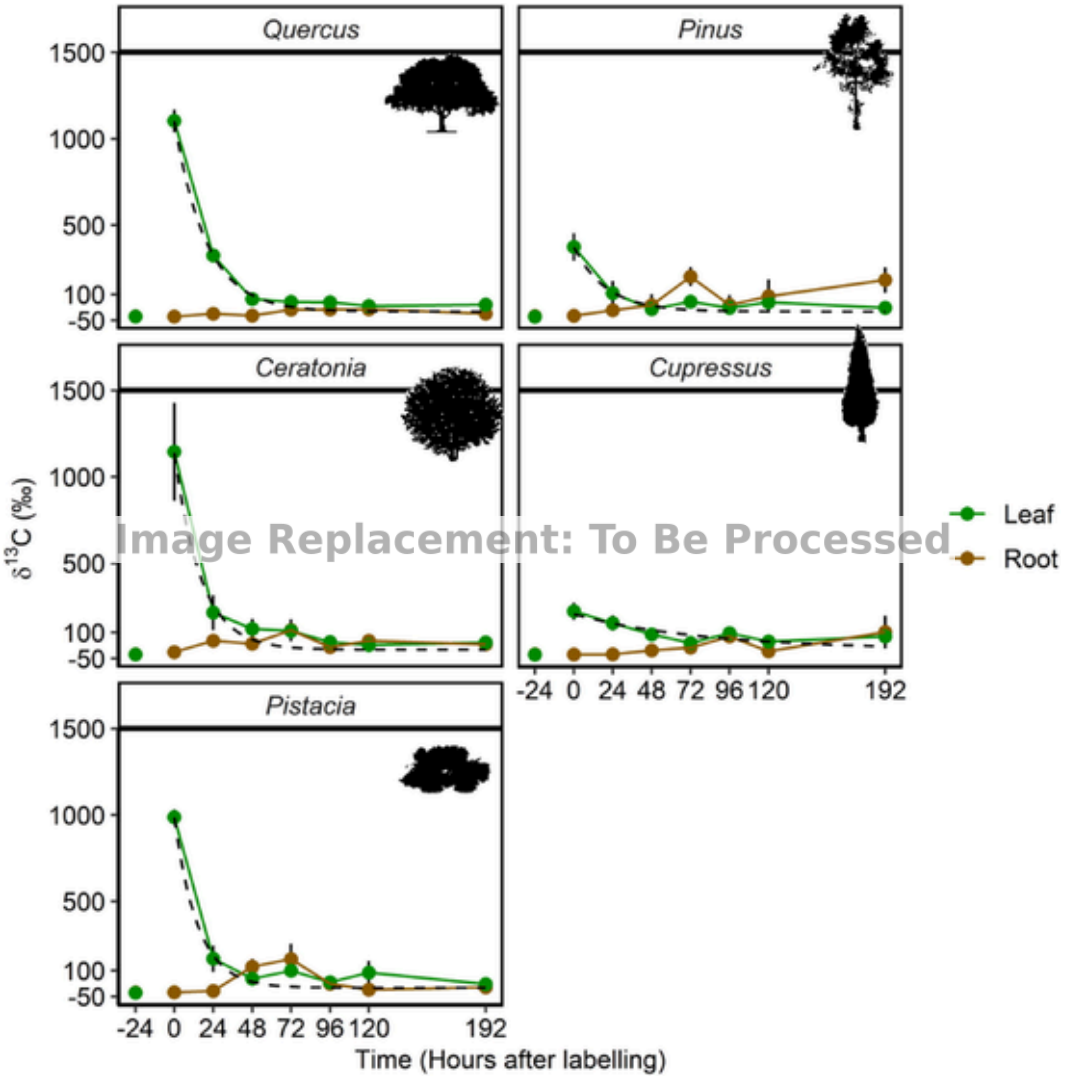

Fig. 2. Evolution of $\delta^{13}C$ in leaf and root biomass following $^{13}CO_2$ labeling of five major Mediterranean forest tree species. Labeled C distributed between leaf biomass (green) and root biomass (brown). Each point represents the mean ± SE of three individual saplings. Dashed lines are the exponential decay of $\delta^{13}C$ of leaves. Woody tissues measurements are not presented. Shapes of mature tree are presented in top right corner of every plot. (For interpretation of the references to colour in this figure legend, the reader is referred to the web version of this article.)

Table 1
Carbon mean residence times (MRT, in hours) in the leaves of five major Mediterranean forest trees days following $^{13}CO_2$ labeling. The two *p-values* (*p*) represent the level of significant of the two variables in the exponential function. The r is the correlation coefficient (Pearson's r) of the exponential model fit.

	Based on measured $\delta^{13}C$				Based on calculated mg C sapling^{-1}			
	MRT	p (N_0)	p (λ)	r	MRT	p (N_0)	p (λ)	r
Pinus	19.31	<0.001	0.008	0.981	41.55	<0.001	0.012	0.94
Cupressus	80.65	<0.001	0.025	0.856	168.29	<0.001	0.063	0.726
Quercus	18.91	<0.001	<0.001	0.998	20.36	<0.001	<0.001	0.996
Ceratonia	15.52	<0.001	0.001	0.995	18.54	<0.001	0.004	0.988
Pistacia	13.82	<0.001	0.003	0.994	19.81	<0.001	0.018	0.974

(paired *t*-test, $t_{14} = -4.58$, *p*-value < 0.001). These differences are typical of woody plants, but are small compared to the increase during label. Imediatelly following the labeling, $\delta^{13}C$ of conifers leaves and fine roots reached 298.3‰ and −25.7‰, respectively, while brodleaf leaves and fine roots reached 1078.7‰ and 22.1‰, respectively (Fig. 2, Table S7). In general, the label was higher in brodleaf leaves compared to conifers needles (*t*-test, $t_7 = 7.09$, *p*-value < 0.001). In addition, ^{13}C signals were higher where the leaf area was lower (i.e. in *Quercus* and *Ceratonia* vs. the other three species). However, ^{13}C signals directly after labelling in the branches were high in conifers and *Pistatica* and neglectable in the other brodleafs (Table S8).

3.3. $\delta^{13}C$ dynamics

During the following days, post labeling, leaf $\delta^{13}C$ decreased and root $\delta^{13}C$ increased, peaking after 72 h (Fig. 2). *Cupressus* was the exception, with more gradual trends in both leaf and root tissues, highlighting the inter-dependence between the tissues. Interestingly, in *Cu-*

pressus and *Pistacia* there was a second, small, delayed leaf enrichment (at 96 and 120 h, respectively) which was not significant. Leaf enrichment was consistently higher than root enrichment in *Quercus*, as well as in the other species mainly during the first days after labelling (Day:Tissue, Repeated-measures, ANOVA, $F_{7,150} = 44.72$, $p < 0.001$, Table S5). However, in *Pinus* 72 h post labeling, the peak root enrichment was ~200‰, almost double the leaf enrichment. Root enrichent showed a second peak after 192 h in conifers but not in brodleafs. The exponential decay of $\delta^{13}C$ (mean values per species) in leaf biomass was fitted to exponential curves (Fig. 2), from which the half-life time and the mean residence time were calculated (Table 1, S8). Modelled exponential curves were statistically significant with the measured data for each species ($p < 0.05$). Half-life times were 9.6–13.1 h in brodleaf and 13.4–55.9 h in conifers. Similarly, mean residence times were 13.8–18.9 h in brodleaf and 19.3–80.65 h in conifers.

3.4. The amount of C allocated to biomass and respiration of leaves and roots

The measured $\delta^{13}C$ signals were transformed into C amounts (mg) using Eqs. (1)–(6), taking advantage of our flux-coupled detection methodology (Fig. 1) and were upscaled to daily values (assuming a stable flux during the day). This quantitative approach further highlighted the differences between leaf and root C allocation. Significant differences were found among leaves and roots in the 8 days of measurements (Day:Tissue, Repeated-measures ANOVA, $F_{7,150} = 44.72$, $p < 0.001$, Table S5). Allocation of C to leaf biomass generally decreased with time across the five tree species (Fig. 3). Allocation of C to roots peaked after 72 h in all species and decreased thereafter, but increased again in *Pinus* and *Cupressus* (Fig. 2). Measured fluxes of respired $^{13}CO_2$ were up-scaled to daily amounts, also expressed as C mass (mg C d^{-1} $sapling^{-1}$) assuming equal fluxes R_{day} and R_{dark}. Allocation of C to leaf respiration was generally in similar timing with allocation to leaf biomass, or delayed by one day in conifers (Fig. 3). Across the five tree species, there was a second, small respiration peak after 144 h. Allocation of C to root respiration showed the most consistent dynamics, with a gradual increase followed by a gradual decrease. Root respiration peak was after 72–96 h in conifers, and after 96–120 h in broadleaf (Fig. 3). As for the leaf $\delta^{13}C$ dynamics, exponential curves were fitted to the C amount curves of leaf biomass pool (Fig. 3), from which the half-life time and the mean residence time were calculated (Table 1, S8). The exponential curves, based on C amounts, were significantly fitted ($p < 0.05$, except of *Cupressus* $p = 0.06$), to the different time points data (Fig. 3) and the values calculated based on the exponential curves were close to those calculated based on the $\delta^{13}C$ data (Fig. 2; Table 1, S8). The mean residence time and half-life of the conifers were double (Table 1, S8) of those of brodleaf parameters. Residuals of the model are observed in the second half of the chase period of the exponential model (Fig. 3, Table S10).

3.5. Dynamics of C partitioning among tree compartments and fluxes

Our three-phase flux-coupled methodology enabled the accurate determination of the fate of assimilated C in space and time. In general, C was gradually moving from biomass to CO_2 (in respiration) and soluble C (in root exudation) (Table S4), and from leaves to woody tissues, and on to roots. During the 8 measurement days post labeling, partitioning to respiration was >28% of assimilated C in *Pinus* (57%), *Quercus* (28%) and *Pistacia* (32%), but only ~16% in the other species (Fig. 4). At the temporal scale of the study, respiration was mostly from the leaves: of the entire respired CO_2 flux, leaf respiration was >70% in all species but *Pistatica*, where respiration from woody tissues was 51% of total respired CO_2. The rest of the respiration was from the roots, with respiration from woody tissues being neglectable except in *Pistatica*. Root exudation accounted for >0.3% of total C in conifers, or less <0.1%, in the other species. The movement of C from leaves to woody tissues and on to roots, was rather consistent in *Ceratonia*, but not in the other species. The partitioning to belowground C allocation on Day 8 was 28–38% in conifers, and much lower in the brodleaf: <10% in *Quercus* and *Ceratonia*, and <5% in *Pistacia* (Figs. 4, 5) (*t*-test, $t_7 = -3.25$, $p = 0.028$). These trends were related to the root/shoot ratios among the tree species, as reflected in their compartment partitioning (Table S1). Root/shoot ratio of brodleaf was higher than that of the conifers (*Quercus* 1.1 ± 0.2, *Ceratonia* 0.5 ± 0.1 and *Pistatica* 0.6 ± 0.2 verses *Pinus* 0.3 ± 0.1 and *Cupressus* 0.4 ± 0.2). *Cupressus* diverged from the other four species in its leaf tissue allocation, which could be partly explained by its high leaf biomass.

3.6. Compartmental model of recent assimilated C distribution in the tree

We employed a compartmental model of C distribution to complement and extend our empirical measurements, and gain a better mechanistic description of the C allocation dynamics. A standard approach in modelling is the use of box-model to describe the kinetics of the labeled C in the different tree compartments (Fig. 1c, Fig. 6; see methods for details). Applying the measured amounts of C after the labelling as the ini-

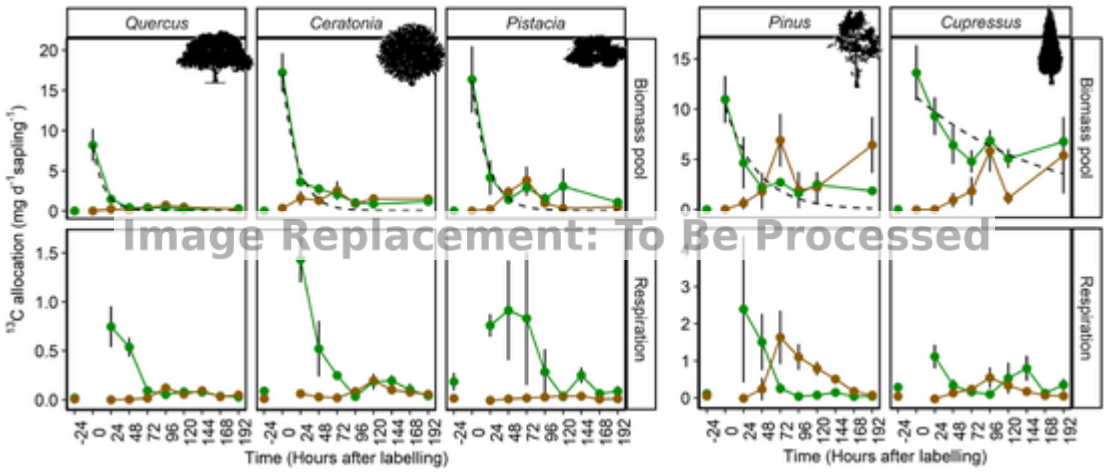

Fig. 3. Allocation of ^{13}C (mg) to biomass pool (top) and respiration (bottom) following $^{13}CO_2$ pulse labeling, in leaves (green) and fine roots (brown) of five major Mediterranean forest tree species. Each point represents the mean ± SE of three individual saplings (small SE are invisible). Dashed lines are the exponential decay of ^{13}C of leaves. Woody tissues measurements are not presented. Shapes of mature tree are presented in top right corner of every plot. (For interpretation of the references to colour in this figure legend, the reader is referred to the web version of this article.)

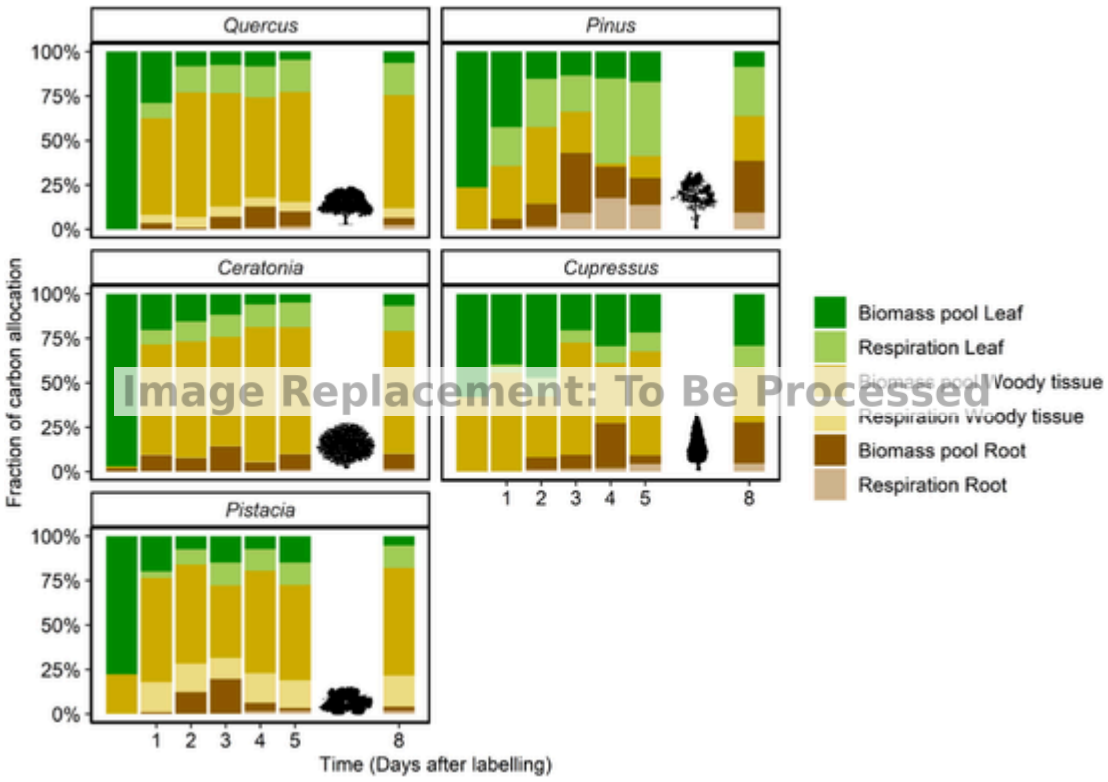

Fig. 4. Three-phase C balance of five major Mediterranean forest tree species along eight days. Internal pools of biomass (dark colors) and external flux of respiration (bright colors) partition to different tree compartments: leaves (green), woody tissues (orange) and fine roots (brown). Each of the three fluxes and three pools was measured independently once a day, except for woody tissues biomass, woody tissues respiration (measured on Day 2 and 5, respectively, and estimated on other days). Each bar represents the mean of three individual saplings, except for woody tissues biomass (1–2 replicates). Shapes of mature tree are presented in every plot. (For interpretation of the references to colour in this figure legend, the reader is referred to the web version of this article.)

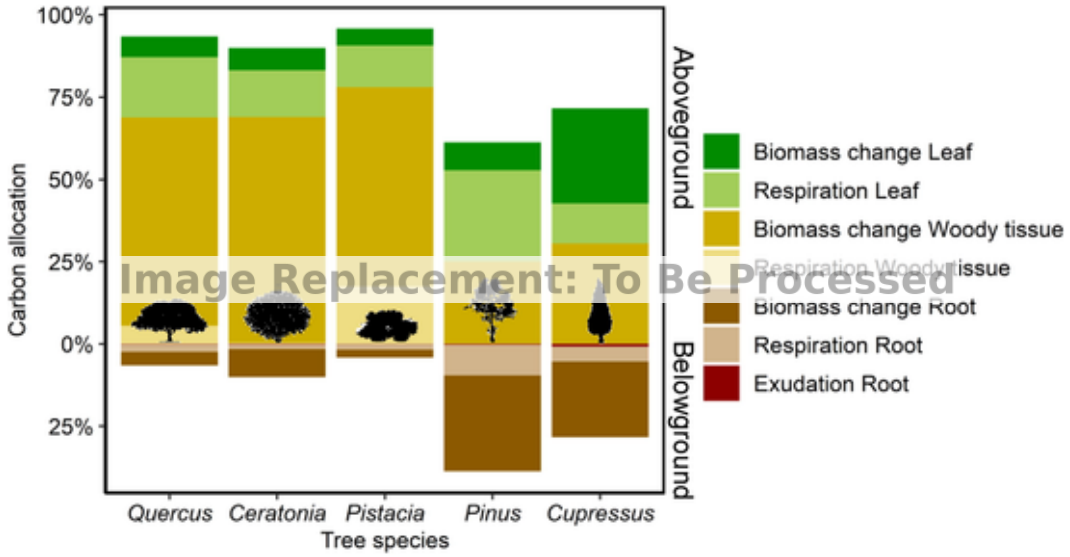

Fig. 5. Aboveground and belowground C pools and fluxes (%) in biomass, respiration and exudation 8 days after labeling of five Mediterranean forest tree species. Internal pools of biomass (dark colors) and external fluxes of respiration (bright colors) and exudation (red) partition to different tree compartments: leaves (green), woody tissues (orange) and roots (brown). Each bar represents the mean of three individual saplings, except for woody tissues biomass and root exudation (1–2 replicates). Shapes of mature tree are presented. (For interpretation of the references to colour in this figure legend, the reader is referred to the web version of this article.)

tial conditions, the calculated rate constants in the model revealed similar C pools dynamics to the measurements. The outputs of our model diverged among tree species (Fig. 6). The model provided continuous resolution of the C allocation dynamics and filled some of the gaps left by the empirical measurements. We observed similar dynamic patterns between the measurements and the model outputs, which confirmed our assumption for linear fluxes among the tree compartments and sinks. The model predicted the C alocation dynamic pattern in the five tree species. However, because of the linear fluxes assumption, the model did not simulate the late belowground C allocation peak in *Pinus* and

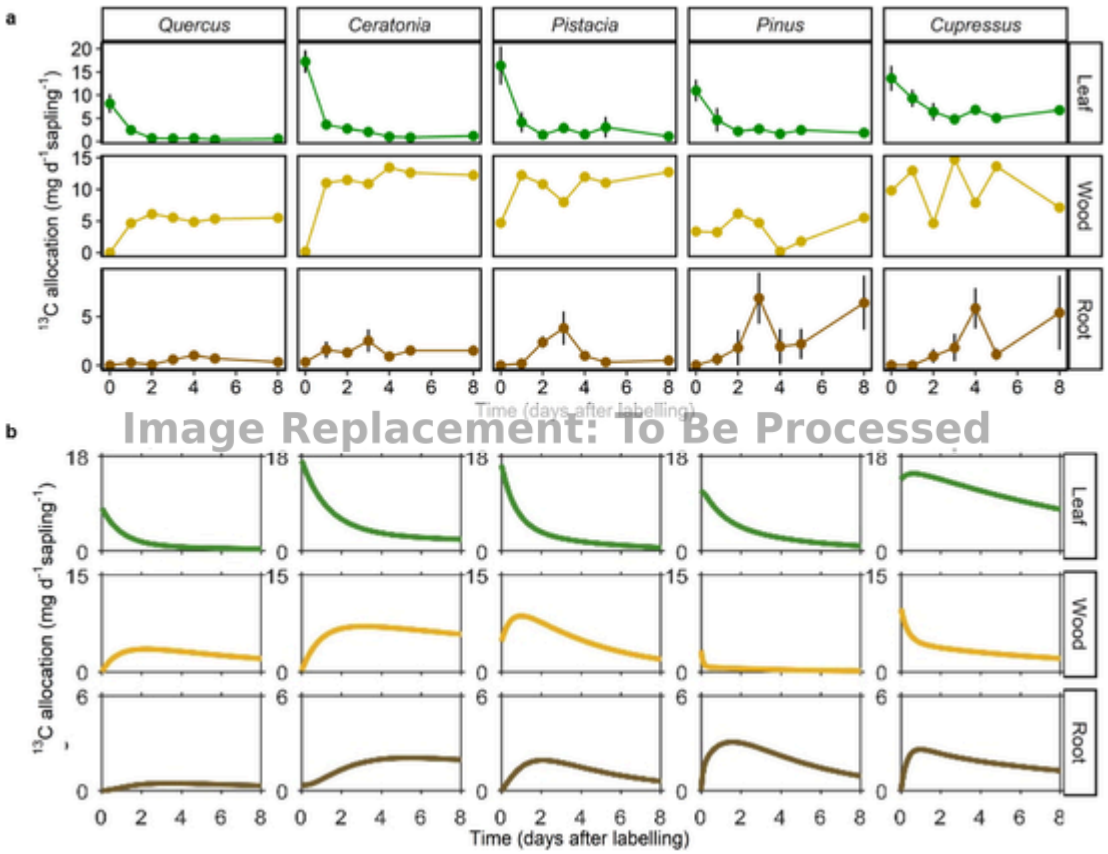

Fig. 6. Empirical results and compartmental model output of C pool dynamics in the tree. **a**. The change of the amount of ^{13}C in the different compartments pools (Leaf, Woody tissues and root) during 8 days post labelling. **b**. Box model outputs of the change of ^{13}C in the different compartments pools dynamics using initial C amounts and rate constants of the measurements. Each point represents the mean of three individual saplings.

Cupressus (Model formulation can not allow such a peak). More discrepancies were found mainly in wood values of *Pinus*, *Cupressus* and *Pistacia*. Finally, we used our model to observe the effect of warming (+5°C and +10 °C) on the respiration fluxes, and thereby on the C allocation dynamics. For a first approximation of warming effects, we included a temperature effect on respiration fluxes. We did not include potential temperature effects on other fluxes. C allocation dynamics were only mildly affected by the higher respiration fluxes (Fig. S5), however the total amount of C allocation to biomass of the different compartments (leaves, woody tissue, roots) were lower (Fig. S5).

4. Discussion

How is C partitioned among tree compartments and sink fluxes in co-occuring Mediterranean tree species? And could these C allocation strategies relate to succession processes or functional groups? Here, we revealed fundamental differences in C allocation between phylogenetically distant tree species (confirming our first hypothesis). In addition, we confirmed our second hypothesis: C partitioning between above- and belowground compartments was significantly different among the five tree species. *Pinus* and *Cupressus* allocated larger amount of C belowground compared with *Quercus*, *Ceratonia* and *Pistacia*. More importantly, we show that measurements on a single species are not transferable to other, co-existing species. In other words, C allocation strategies diverge among tree species within an ecosystem.

4.1. Integrated pulse labeling and C mass balance

Pulse-labeling of trees has been a major approach for studying their C allocation dynamics for the past thirty years (Schneider and Schmitz, 1989; Epron et al., 2012). The results of those studies shaped our understanding of the rate of transfer of assimilated C to tree compartments. At the same time, the use of a C mass balance approach complemented these observations, especially for mature trees and temporal sclaes longer than, e.g., a month (Klein and Hoch, 2015). This study attempts, for the first time, to combine these two approaches into a powerfull, hollistic view of tree C allocation. It is unique in (i) combining continuous measurements of C flux and ^{13}C enrichment, permitted by coupling of continuous ^{13}C detection with IRGA CO_2 gas analysis; (ii) tracing the labeled C in solid, liquid, and gas forms simultaneously (including root exudation); and (iii) integrating the data collected based on (i) and (ii) above into a whole-tree mass balance. In addition, to the best of our knowledge, this is the first study of detailed C allocation dynamics of (iv) Mediterranean tree species, and (v) simultaneously performed on five tree species. Overall, the main strength of our setup is the ability to couple fluxes and pool measurements which improves our understanding of C allocation in different tree species and environmental conditions.

4.2. Limitations and advantages of our approach

For calculating a whole tree C balance, several assumptions and simplifications were taken. First, saplings were divided into three main compartments, which presented C allocation differences in the short time scale of days (Figs. 3 & 4). However, a higher resolution measurement of C dynamics, e.g. by separating the root system into coarse and fine roots, can expose significant differences within the root system (Wegener et al., 2015). Second, our assumption of constant pools and fluxes dynamics during 24 h, relying on a single time-point prevented a finer temporal scale onservation. Nevertheless, we did correct for the respiration dependence on temperature, using the current daily temperature (Fig. S3, Table S3), and Q_{10} values (Atkin and Tjoelker, 2003)

post labeling (Fig. 3, Fig. 4). Because of the short time scale (8 days) and the relatively slow growth of these Mediterranian species, specifically in the dry season (when the mesurements took place), neglectable growth was assumed. In addition, the measurements took place in a certain plant phenology (i.e. mid-summer) and the C allocation strategies are accurate for this time of the phenology alone. Furthermore, the measurement were only for 8 days, which the allocation patterns may have extended or even increased mainly regarding the C allocation to roots (Fig. 3). Our approach offerred some notable advantges: Saplings compartments were measured directly, without assumptions on rhizosphere respiration ratio (i.e autotrophic versus heterotrophic), since root respiration and root exudation were measured directly (Fig. 4). In addition, the mass balance calculation approach is based on the exact area and mass of the different measured plant compartments and the total sapling. Last, a verification of our pool and flux calculation was made by comparing the total amount of labeled C in the sapling by assimilation flux and the total pool of C present in biomass post labeling (Fig. S4). Future experiments, including measurements of all pools and fluxes (without estimations to fill the gaps), will also include recovery rates, and will better inform our understanding of C allocation mechanisms.

4.3. Carbon allocation dynamics using a compartmental model

The compartmental model of C allocation dynamics (Epron et al., 2012) makes a better mechanistic description of the highly complex tree system, and it can be used to extend the results and predicts the effects of other environmental conditions (e.g., temperature) that were not tested directly. We observed similar C allocation dynamics between the measurements and our model outputs (Fig. 6). The main discrepancies are in the wood compartment, probably because this was the only compartment that was not measured directly in all days, and was calculated using the mass balance approach. The model predicted lower allocation belowground in conifers and similar amounts in broadleaves. This gap is probably because the late C allocation flux is not part of the linear dynamic (which was part of the model assumptions) and is species-specific or specific to conifers or early succession species. This high belowground investment can be explained by the “second peak” in the root pools and fluxes, which was not predicted by the model (Figs. 4 & 6). Double peaks in belowground C allocation after pulse labelling experiments were observed in other resource-limited conditions (Barthel et al., 2011; Wegener et al., 2015). Interestingly, the belowground investment of conifers is also partially sensitive to high temperature (Fig. S5). Under warming scenarios, our model predicted lower C allocation to biomass and higher C amount in the atmospheric and soil sinks (Fig. S5). This can be explained by an increase in the transfer time of belowground C (Blessing et al., 2015). This result supports the varied effects of temperature on C allocation dynamics and the interactions with plant respiration (Atkin and Tjoelker, 2003) and metabolic rates (Blessing et al., 2015) or species origin (Way and Oren, 2010). Also, contributing to the unique C allocation dynamics, we observed the high C allocation plasticity of the Mediterranean species (Zunzunegui et al., 2005; Wegener et al., 2015), and the limited nutrients in the soil which forces faster micobial interactions in the early successional species.

4.4. C allocation dynamics in various functional groups of trees

Published C allocation studies typically focused on 1–2 species, with four species the maximum number so far (Ghirardo et al., 2010). Here, the inclusion of five species offered an opportunity to test for interspecific differences. Among such differences, the major divergence was between two groups of trees, *Pinus* and *Cupressus* vs. *Quercus*, *Ceratonia* and *Pistacia*. These two groups can be separated by their functional group for conifers vs. broadleavs, respectively. In contrast to broadleaves, conifers showed (i) a second root C allocation peak on Day 8; (ii) sustained root C allocation; (iii) higher mean residence time in leaves; and (iv) higher partitioning of C allocation belowground (Fig. 4). Based on data from 47 pulse labeling studies, Epron et al. (2012) concluded that the label transfer rate from leaves to soil was, on average, an order of magnitude lower in conifer vs. broadleaf species. Differences in phloem anatomy between conifer and broadleaf (Jensen et al., 2012) can indicate a longer retention time of C in a given tissue. It is hence possible, that the higher allocation to fine roots in conifer is unrelated to transfer rates through the phloem tissue (which are probably higher in broadleaf), but rather, to longer retention in fine roots in conifer vs. broadleaf. Another possible explanation considers one of the implications of the so-called ‘pot binding effect’ on the conifers in our study. It is possible that *Pinus* and *Cupressus* saplings reached the maximum height allowed by the pot size (Fig. S1), however, a similar root mass fraction (~40%) was found in larger pots of the same *Pinus* specie. In summary, belowground C allocation was higher in conifer than in broadleaf but the exact mechanism is yet to be unraveled.

4.5. Ecological strategy influence tree C allocation

Why conifer saplings allocate more C belowground than broadleaf saplings? The similarities between the pot experiment and a mixed forest go beyond the tree species identity. The five Mediterenean species we studied partitioned in the same way along the conifers versus broadleaf divide and early versus late succession species. The conifers, which are the early succession species among the five species (Sheffer, 2012), invest more C belowground (Fig. 5), probably because of the faster establishment strategy (Shukla and Ramakrishnan, 1984; Gleeson and Tilman, 1994). Because we grew the plants with forest soil (that has limited nutrients) and unlimited light we can assume the limiting factor was belowground. Both limitations have been shown to affect C alocation (Wegener et al., 2015). The late sucssion species, *Quercus*, *Ceratonia* and *Pistacia,* were found to invest more C in the woody tissues, consistent with their shade tolerance and longer life cycle properties (Fig. 5). Thus, the differences in C allocation strategies can be explained in part by succession growth characteristics. However, the five tree species are seperated to functional group and succssional charecteristic in the same way, thus understanding this phenomenas would requier further research including more tree species, e.g. an early succession broadleaf species.

4.6. Root exudation and its proportion in the C balance

Root exudation fluxes are relatively small. Nonetheless, they provide important contribution to our understanding of tree C allocation and species-specific strategies. Root exudation flux (Phillips et al., 2008) together with root exudation composition (Gargallo-Garriga et al., 2018) are affected by a variety of environmental parameters, can be plant-specific (Grayston et al., 1997) and successional stage related (Sun et al., 2021). Root exudation accounted for 0.7% of total C in *Cupressus*, and less in the other species (Fig. 5). In addition, *Cupressus* C allocation into root biomass is high while root respiration flux is low (Fig. 3). This high C allocation to the roots that maintain low respiration flux and high exudation rate might suggest that the high belowground investment is directed to root exudations. In addition, this high exudation flux is in line with the relatively high exudation rate found in the same species (i.e. *Cupressus* and *Pistacia*) in a mature forest (Jakoby et al., 2020). Furthermore, this potted experiment took place in midsummer, which is the time of the high exudation flux detected in the forest. The early successional species are known to exude higher quantities of C than the late-successional species (Sun et al., 2021), potentially for stimulating microbial communities and improving nutrient availability. The low but significant root exudation flux underscores the need for more research into exudation mechanisms and their importance to the functional and ecological strategies used by trees. Our mass balance, pulse labeling, and compartmental model setup promises to

expand our capabilities to understand the exudation flux in many species and plant types.

5. Conclusions

Carbon allocation dynamics research in a mixed forest requires quantification at the individual tree scale with compartment resolution. By combining pulse labeling, mass balance, and compartmental model, we quantified C allocation dynamics in five tree species, representing contrasting functional types and successional stages. C allocation strategies diverged among tree species co-habiting in a typical Mediterranean forest. Within 8 days, conifers allocated 30% of the C belowground, and broadleaves allocated <10%. This belowground investment could be explained by the early successional stage of the conifers. However, further research using broadleaves which are also early succession species is needed. Root exudation fluxes were small but significant and are in agreement with the ecological niche of the entire C allocation strategy (mainly in *Cupressus*). Our unique setup could be used in potted experiments as well as mature trees and should allow to extrapolate the fluxes that cannot be quantified directly. Such application will lead to better understanding of forest tree C allocation dynamics and the inputs of environmental factors.

Declaration of Competing Interest

The authors declare that they have no known competing financial interests or personal relationships that could have appeared to influence the work reported in this paper.

Acknowledgements

The authors thank Prof. Dan Yakir for the compartmental model comments and suggestions. Special thanks go to Dr. Ron Milo (WIS, Israel), Dr. Nadine Ruehr (KIT, Germany), Raphael Weber (University of Basel, Switzerland) and Dr. Stav Livne-Luzon (WIS, Israel) for providing useful feedback on an earlier version of this manuscript. Root exudation measurement technique followed the method used by Hilla Gil and Prof. Shimon Rachmilevitch of Ben Gurion University, Israel. Shacham Megidish and Rotem Cahanovitc are acknowledged for lab assistance and Gily Ginosar for the model programing design. We thank Prof. Asaph Aharoni for providing the labeling chamber. The authors thank the Merle S. Cahn Foundation; the Monroe and Marjorie Burk Fund for Alternative Energy Studies; Mr. and Mrs. Norman Reiser; the Weizmann Center for New Scientists; the estate of Helen Nichunsky; the Benoziyo Endowment Fund for the Advancement of Science; and the Edith & Nathan Goldberg Career Development Chair. The project was funded in part by the European Research Council project RHIZOCARBON, granted to TK. IR is supported by the Sustainability and Energy Research Initiative Ph.D. Fellowship.

Appendix A. Supplementary material

Supplementary data to this article can be found online at https://doi.org/10.1016/j.foreco.2021.119258.

References

Alessandri, A., De Felice, M., Zeng, N., Mariotti, A., Pan, Y., Cherchi, A., Lee, J.Y., Wang, B., Ha, K.J., Ruti, P., Artale, V., 2014. Robust assessment of the expansion and retreat of Mediterranean climate in the 21st century. Sci. Rep. 4, 7211.

Atkin, O.K., Tjoelker, M.G., 2003. Thermal acclimation and the dynamic response of plant respiration to temperature. Trends Plant Sci. 8, 343–351.

Barthel, M., Hammerle, A., Sturm, P., Baur, T., Gentsch, L., Knohl, A., 2011. The diel imprint of leaf metabolism on the δ13C signal of soil respiration under control and drought conditions. New Phytol. 192, 925–938.

Blessing, C.H., Werner, R.A., Siegwolf, R., Buchmann, N.J.T.p., 2015. Allocation dynamics of recently fixed carbon in beech saplings in response to increased temperatures and drought. 35, 585–598.

Bonet, A., 2004. Secondary succession of semi-arid Mediterranean old-fields in south-eastern Spain: insights for conservation and restoration of degraded lands. J. Arid Environ. 56, 213–233.

Brant, J.B., Myrold, D.D., Sulzman, E.W.J.O., 2006. Root controls on soil microbial community structure in forest soils. 148, 650–659.

Coplen, T.B., 2011. Guidelines and recommended terms for expression of stable-isotope-ratio and gas-ratio measurement results. Rapid Commun. Mass Spectrom. 25, 2538–2560.

Dannoura, M., Maillard, P., Fresneau, C., Plain, C., Berveiller, D., Gerant, D., Chipeaux, C., Bosc, A., Ngao, J., Damesin, C.J.N.P., 2011. In situ assessment of the velocity of carbon transfer by tracing 13C in trunk CO 2 efflux after pulse labelling: variations among tree species and seasons. 190, 181–192.

Delipetrou, P., Makhzoumi, J., Dimopoulos, P., Georghiou, K., 2008. Cyprus. In: Mediterranean Island Landscapes. Springer, pp. 170–203.

Desalme, D., Priault, P., Gérant, D., Dannoura, M., Maillard, P., Plain, C., Epron, D., 2017. Seasonal variations drive short-term dynamics and partitioning of recently assimilated carbon in the foliage of adult beech and pine. New Phytol. 213, 140–153.

Dormand, J.R., Prince, P.J., 1980. A family of embedded Runge-Kutta formulae. J. Comput. Appl. Math. 6, 19–26.

Enquist, B.J., Niklas, K.J., 2002. Global allocation rules for patterns of biomass partitioning in seed plants. Science 295, 1517–1520.

Epron, D., Bahn, M., Derrien, D., Lattanzi, F.A., Pumpanen, J., Gessler, A., Hogberg, P., Maillard, P., Dannoura, M., Gerant, D., Buchmann, N., 2012. Pulse-labelling trees to study carbon allocation dynamics: a review of methods, current knowledge and future prospects. Tree Physiol. 32, 776–798.

Epron, D., Ngao, J., Dannoura, M., Bakker, M., Zeller, B., Bazot, S., Bosc, A., Plain, C., Lata, J., Priault, P., 2011. Seasonal variations of belowground carbon transfer assessed by in situ 13 CO 2 pulse labelling of trees. Biogeosciences 8, 1153–1168.

Farquhar, G.D., Busch, F.A., 2017. Changes in the chloroplastic CO2 concentration explain much of the observed Kok effect: a model. New Phytol. 214, 570–584.

Franklin, O., Johansson, J., Dewar, R.C., Dieckmann, U., McMurtrie, R.E., Brännström, Å., Dybzinski, R., 2012. Modeling carbon allocation in trees: a search for principles. Tree Physiol. 32, 648–666.

Gargallo-Garriga, A., Preece, C., Sardans, J., Oravec, M., Urban, O., Peñuelas, J., 2018. Root exudate metabolomes change under drought and show limited capacity for recovery. Sci. Rep. 8, 1–15.

Ghirardo, A., Koch, K., Taipale, R., Zimmer, I., Schnitzler, J.P., Rinne, J., 2010. Determination of de novo and pool emissions of terpenes from four common boreal/alpine trees by 13CO2 labelling and PTR-MS analysis. Plant, Cell Environ. 33, 781–792.

Giorgi, F., Lionello, P., 2008. Climate change projections for the Mediterranean region. Global Planet. Change 63, 90–104.

Gleeson, S., Tilman, D., 1994. Plant allocation, growth rate and successional status. Funct. Ecol. 543–550.

Grayston, S., Vaughan, D., Jones, D., 1997. Rhizosphere carbon flow in trees, in comparison with annual plants: the importance of root exudation and its impact on microbial activity and nutrient availability. Appl. Soil Ecol. 5, 29–56.

Hagedorn, F., Joseph, J., Peter, M., Luster, J., Pritsch, K., Geppert, U., Kerner, R., Molinier, V., Egli, S., Schaub, M., Liu, J.F., Li, M., Sever, K., Weiler, M., Siegwolf, R.T., Gessler, A., Arend, M., 2016. Recovery of trees from drought depends on belowground sink control. Nat. Plants 2, 16111.

Högberg, P., Högberg, M., Göttlicher, S., Betson, N., Keel, S., Metcalfe, D., Campbell, C., Schindlbacher, A., Hurry, V., Lundmark, T.J.N.P., 2008. High temporal resolution tracing of photosynthate carbon from the tree canopy to forest soil microorganisms. 177, 220–228.

Jakoby, G., Rog, I., Megidish, S., Klein, T., 2020. Enhanced root exudation of mature broadleaf and conifer trees in a Mediterranean forest during the dry season. Tree Physiol. 40, 1595–1605.

Jensen, K.H., Liesche, J., Bohr, T., Schulz, A., 2012. Universality of phloem transport in seed plants. Plant, Cell Environ. 35, 1065–1076.

Keel, S.G., Siegwolf, R.T., Korner, C., 2006. Canopy CO2 enrichment permits tracing the fate of recently assimilated carbon in a mature deciduous forest. New Phytol. 172, 319–329.

Klein, T., Hoch, G., 2015. Tree carbon allocation dynamics determined using a carbon mass balance approach. New Phytol. 205, 147–159.

Klein, T., Vitasse, Y., Hoch, G., 2016. Coordination between growth, phenology and carbon storage in three coexisting deciduous tree species in a temperate forest. Tree Physiol. 36, 847–855.

Kuptz, D., Fleischmann, F., Matyssek, R., Grams, T.E.J.N.P., 2011. Seasonal patterns of carbon allocation to respiratory pools in 60-yr-old deciduous (Fagus sylvatica) and evergreen (Picea abies) trees assessed via whole-tree stable carbon isotope labeling. 191, 160–172.

Maestre, F.T., Cortina, J., Bautista, S., 2004. Mechanisms underlying the interaction between Pinus halepensis and the native late-successional shrub Pistacia lentiscus in a semi-arid plantation. Ecography 27, 776–786.

Merganičová, K., Merganič, J., Lehtonen, A., Vacchiano, G., Sever, M.Z.O., Augustynczik, A.L., Grote, R., Kyselová, I., Mäkelä, A., Yousefpour, R., 2019. Forest carbon allocation modelling under climate change. Tree Physiol. 39, 1937–1960.

Ne'eman, G., Izhaki, I., 1996. Colonization in an abandoned East-Mediterranean vineyard. J. Veg. Sci. 7, 465–472.

Parr, R.M., Clements, S., 1991. Intercomparison of enriched stable isotope

reference materials for medical and biological studies. International Atomic Energy Agency.
Phillips, R.P., Erlitz, Y., Bier, R., Bernhardt, E.S.J.F.E., 2008. New approach for capturing soluble root exudates in forest soils. 22, 990–999.
Poorter, H., Niklas, K.J., Reich, P.B., Oleksyn, J., Poot, P., Mommer, L., 2012. Biomass allocation to leaves, stems and roots: meta-analyses of interspecific variation and environmental control. New Phytol. 193, 30–50.
Rueden, C.T., Schindelin, J., Hiner, M.C., DeZonia, B.E., Walter, A.E., Arena, E.T., Eliceiri, K.W., 2017. Image J2: ImageJ for the next generation of scientific image data. BMC Bioinf. 18, 529.
Ruehr, N.K., Offermann, C.A., Gessler, A., Winkler, J.B., Ferrio, J.P., Buchmann, N., Barnard, R.L.J.N.P., 2009. Drought effects on allocation of recent carbon: from beech leaves to soil CO2 efflux. 184, 950–961.
Sala, A., Woodruff, D.R., Meinzer, F.C., 2012. Carbon dynamics in trees: feast or famine?. Tree Physiol. 32, 764–775.
Sangster, A., Knight, D., Farrell, R., Bedard-Haughn, A., 2010. Repeat-pulse 13CO2 labeling of canola and field pea: implications for soil organic matter studies. Rapid Commun. Mass Spectrom. 24, 2791–2798.
Schneider, A., Schmitz, K.J.T., 1989. Seasonal course of translocation and distribution of 14 C-labelled photoassimilate in young trees of Larix decidua Mill. 3, 185–191.
Schnyder, H., Schäufele, R., Lötscher, M., Gebbing, T., 2003. Disentangling CO2 fluxes: Direct measurements of mesocosm-scale natural abundance $^{13}CO_2/^{12}CO_2$ gas exchange, 13C discrimination, and labelling of CO_2 exchange flux components in controlled environments. Plant, Cell Environ. 26, 1863–1874.
Shampine, L.F., Reichelt, M.W., 1997. The matlab ode suite. SIAM J. Sci. Comput. 18, 1–22.
Sheffer, E., 2012. A review of the development of Mediterranean pine–oak ecosystems after land abandonment and afforestation: are they novel ecosystems?. Ann. Forest Sci. 69, 429–443.
Shukla, R., Ramakrishnan, P., 1984. Biomass allocation strategies and productivity of tropical trees related to successional status. For. Ecol. Manage. 9, 315–324.
Streit, K., Rinne, K.T., Hagedorn, F., Dawes, M.A., Saurer, M., Hoch, G., Werner, R.A., Buchmann, N., Siegwolf, R.T., 2013. Tracing fresh assimilates through Larix decidua exposed to elevated CO(2) and soil warming at the alpine treeline using compound-specific stable isotope analysis. New Phytol. 197, 838–849.
Sun, L., Ataka, M., Han, M., Han, Y., Gan, D., Xu, T., Guo, Y., Zhu, B., 2021. Root exudation as a major competitive fine-root functional trait of 18 coexisting species in a subtropical forest. New Phytol. 229, 259–271.
Team, R.C., 2018. R: A Language and Environment for Statistical Computing. In. R Foundation for Statistical Computing, Vienna, Austria.
Verkouteren, R., 2006. New guidelines for δ13C measurements. Anal. Chem. 78.
Way, D.A., Oren, R., 2010. Differential responses to changes in growth temperature between trees from different functional groups and biomes: a review and synthesis of data. Tree Physiol. 30, 669–688.
Wegener, F., Beyschlag, W., Werner, C., 2015. High intraspecific ability to adjust both carbon uptake and allocation under light and nutrient reduction in Halimium halimifolium L. Front. Plant Sci. 6, 609.
Wilson, J.B., 1988. A review of evidence on the control of shoot: root ratio, in relation to models. Ann. Bot. 61, 433–449.
Zunzunegui, M., Barradas, M.D., Ain-Lhout, F., Clavijo, A., Novo, F.G., 2005. To live or to survive in Doñana dunes: adaptive responses of woody species under a Mediterranean climate. Plant Soil 273, 77–89.